Theoretical Study on Molecular Structure and Electronic Properties of New 1,3-Diaza-adamantan-6-ones Derivatives

Haithem Abdulhasan, Ahmed Al-Yasari*, and Rahman Alasadi

University of Kerbala, P.O. Box 1125, Kerbala, Iraq

* ***Corresponding author:***

tel: +96432-7729137527
email: a.alyasari@uokerbala.edu.iq

Received: March 22, 2019
Accepted: May 14, 2019

DOI: 10.22146/ijc.44403

Abstract: *In this study, the structural geometry and vibrational frequencies (IR) of 1,3-Diaza-adamantane-6-ones derivatives including Adamantane (**A**), 1,3-Diaza-adamantan (**D**), 1,3-Diaza-adamantan-6-one (**DO**), 5-Benzyl-1,3-diaza-adamantan-6-one (**BD**), 5-(4-Hydroxybenzyl)-1,3-diaza-adamantan-6-one (**HBD**), 5-(4-Methoxy benzyl)-1,3-diaza-adamantan-6-one (**MBD**), and 5-(4-Hydroxy-3-methoxybenzyl)-1,3-diaza-adamantan-6-one (**HMBD**) were theoretically studied. In addition, molecular orbital energies, including the highest occupied molecular orbitals (HOMOs), and lowest unoccupied molecular orbitals (LUMOs), and electronic properties of the titled molecules were theoretically studied using the computational method. Optimized molecular structures were obtained by DFT method with the hybrid B3LYP functional at a relatively small basis set of 6-31G. The calculated vibrational wavenumbers were obtained using the same level of the theory mentioned above. The contributions to the molecular orbitals of adamantane and substituted-phenyl groups in the title compounds were determined. Moving from **A** to **HMBD**, a decrease in the value of LUMO and total energy are noticed, while an increase in the value of HOMO is noted. These findings are supported by the decrease in the $E_{HOMO-LUMO}$ gap values. Furthermore, a decrease in the value of ionization potential (IP) is obtained, while an increase in the electron affinity (EA) is observed.*

Keywords: *Adamantane; 1,3-Diaza-adamantan; DFT/B3LYP*

■ INTRODUCTION

Adamantane and its derivatives have fascinating structures due to their various physiological, pharmaceutical, and medical activities [1-6]. It consists of a polycyclic cage molecule with high symmetry representing diamondoids–hydrogen-terminated hydrocarbons with a diamond-like structure [7-8]. Among these derivatives, 1,3-Diaza-adamantane derivatives have attracted great attention due to their interesting properties [9] such as antibacterial, and psychotropic activity [10-11]. Sharabi-Ronen et al. have reported the anti-neoplastic activity of 1,3-Diaza-2-functionalized-adamantan-6-one compounds against melanoma cells [12]. They showed that the ability of the reported compounds to introduce apoptosis in melanoma cells was significant.

1,3-Diazaadamantane-6-one derivatives have attracted considerable attention for diverse applications. Recently, we reported the synthesis of a new series of 1,3-Diaza-adamantane-6-ones derivatives [13]. However, their structural geometry and vibrational properties have not been studied yet. To the best of our knowledge, the quantum chemical calculations on these derivatives have not been done so far. In this study, the molecular structure and the full vibrational spectra have been reported. Moreover, the effect of substitution on electronic properties such as the ionization potential, the electron affinity, electronegativity, and the energy gap between HOMO–LUMO are generally studied.

■ COMPUTATIONAL METHODS

All computational procedures were carried out using GAMESS and Avogadro 1.1.1 [14-15]. The optimization structure of Adamantane (**A**), including 1,3-Diaza-adamantan (**D**), 1,3-Diaza-adamantan-6-one (**DO**), 5-Benzyl-1,3-diaza-adamantan-6-one (**BD**), 5-(4-Hydroxybenzyl)-1,3-diaza-adamantan-6-one (**HBD**), 5-

(4-Methoxybenzyl)-1,3-diaza-adamantan-6-one (**MBD**) and 5-(4-Hydroxy-3-methoxybenzyl)-1,3-diaza-adaman tan-6-one (**HMBD**) molecules have been performed using DFT method with the hybrid B3LYP functional at 6-31G level in the gas phase. The applied method is a combination of the Hartree–Fock method and the density functional theory using Becke's three parameter (B3) gradient corrected functionals [15] and Lee–Yang exchange-correlation functional (LYP) [16]. Molecular geometries of all systems were fully optimized at the B3LYP functional with a relatively small basis set of 6-31G level of theory. The stationary points determined with geometry optimization with minimal energy was confirmed by calculating the normal vibration frequencies with the use of second derivatives at the same level of theory. The energy gap ($E_{HOMO\text{-}LUMO}$ gap), Ionization potential (IP), electron affinity (EA), and the electronegativity (X) have been calculated using equations 1, 2, 3, 4, respectively.

$$E_{HOMO-LUMO}\ \text{gap} = E_{LUMO} - E_{HOMO} \quad (1)$$

$$IP = -E_{HOMO} \quad (2)$$

$$EA = -E_{LUMO} \quad (3)$$

$$X = -0.5\left(E_{HOMO} + E_{LUMO}\right) \quad (4)$$

Both the vibrational modes and frequencies were assigned, and the animations of normal modes were visualized by using Avogadro 1.1.1 [17].

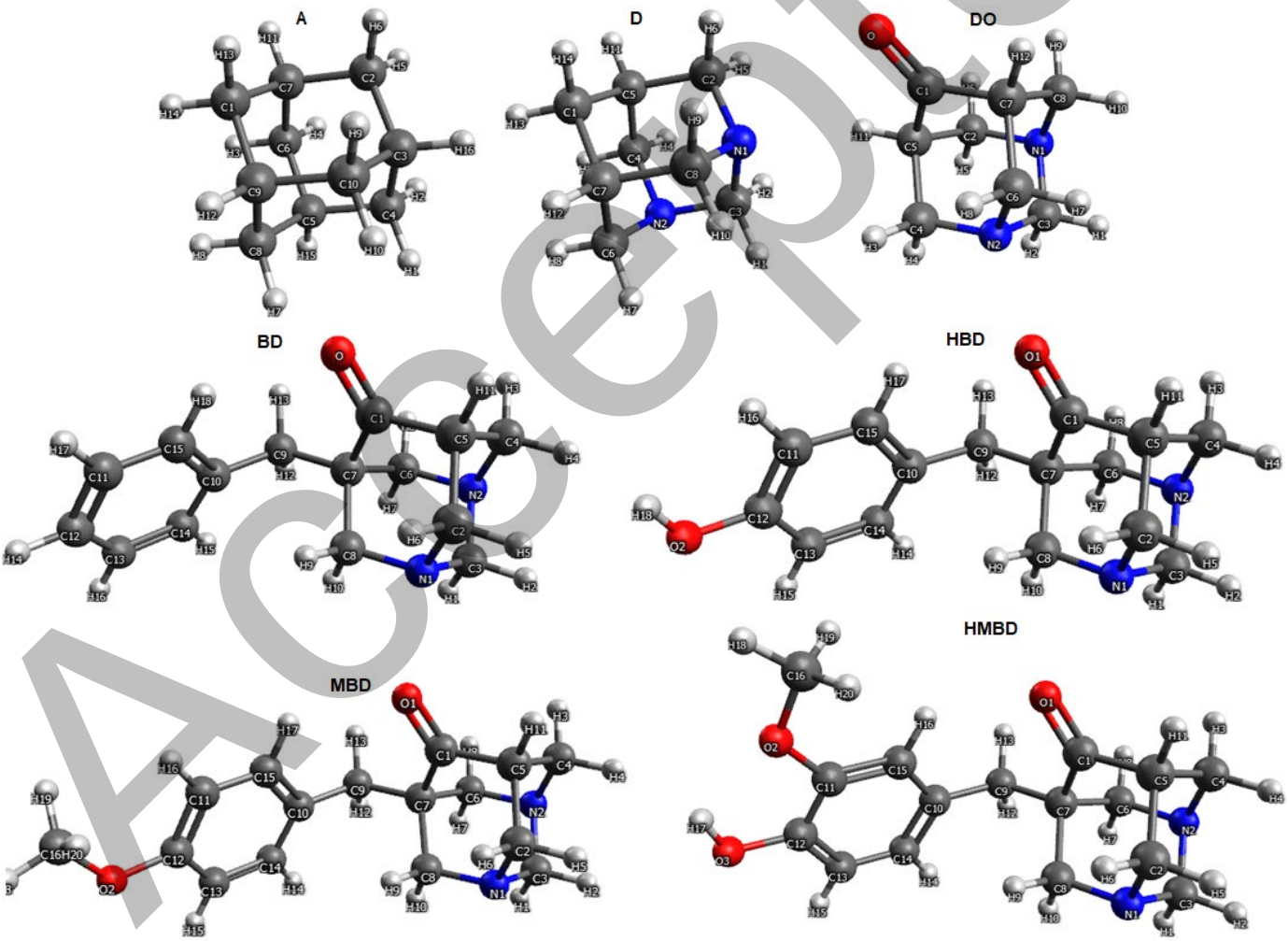

Fig 1. The optimized structure of molecules **A**, **D**, **DO**, **BD**, **HBD**, **MBD**, and **HMBD**

■ RESULTS AND DISCUSSION

Molecular Geometric Structure

The chemical reactivity and hence, the chemical properties are affected by the change in molecular structure. Therefore, the effect of substitution of 1,3-diaza-adamantan derivatives with their parent Adamantane (**A**), including 1,3-Diaza-adamantan (**D**), 1,3-Diaza-adamantan-6-one (**DO**), 5-Benzyl-1,3-diaza-adamantan-6-one (**BD**), 5-(4-Hydroxybenzyl)-1,3-diaza-adamantan-6-one (**HBD**), 5-(4-Methoxybenzyl)-1,3-diaza-adamantan-6-one (**MBD**) and 5-(4-Hydroxy-3-methoxybenzyl)-1,3-diaza-adamantan-6-one (**HMBD**) have been studied.

Fig. 1 shows the geometric structures of the as-studied molecules as obtained by calculations. Selections of the most important structural parameters of all molecules are listed in Table 1, and the full details of geometric parameters may be obtained from the author upon request. By considering the data for compound **A** and **D**, upon the substitution of two carbon by two nitrogen, the latter showed an increase in the angle value of N1-C3-N2 due to the effect of lone pair in the nitrogen of the heteroatom. Generally, in all compounds, N-C-N angles are slightly wider than C-N-C angles. In the case of compound **HMBD**, the bond length of C12-O2 is shorter than that in compound **MBD**, but the length of O3-C16 is longer. The C7-C9-C10 angle is slightly wider compared with compound **MBD**, and noticeably wider than the other studied compounds.

The same trend was noticed for the value of C5-C1-C7. The C4-N2-C6 showed a slight increase in its value when moving from compound **D** to **HMBD**. The

Table 1. Selected geometric parameters (bond distances, Å, bond and torsion angles, °) of **A**, **D**, **DO**, **BD**, **HBD**, **MBD**, and **HMBD**

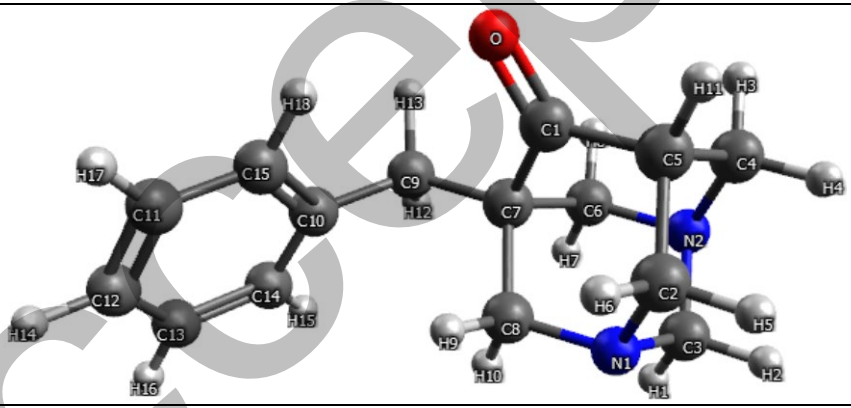

Compound	A	D	DO	BD	HBD	MBD	HMBD
N1-C3-N2 (°)	109.7*	112.6	113	111.6	111.6	111.6	111.6
C2-N1-C8 (°)	-	109.8	109.9	110.2	110.1	110.1	110.2
C4-N2-C6 (°)	-	109.8	109.9	110.3	110.3	110.3	110.3
N1-C2 (Å)	-	1.494	1.464	1.482	1.482	1.483	1.481
N1-C3 (Å)	-	1.488	1.466	1.482	1.482	1.482	1.482
N2-C3 (Å)	-	1.488	1.466	1.486	1.486	1.486	1.486
C5-C1-C7 (°)	109.7”	108.6	110.7	113	112.9	112.9	113
C1-O1 (Å)	-	-	1.213	1.248	1.248	1.248	1.249
C7-C9-C10 (°)	-	-	-	116.5	116.4	117	117.2
C7-C9 (Å)	-	-	-	1.551	1.550	1.548	1.550
C9-C10 (Å)	-	-	-	1.521	1.522	1.522	1.522
C12-O2 (Å)	-	-	-	-	1.395	1.394	1.387
O3-C16 (Å)	-	-	-	-	-	1.451	1.453

In case of A, * = C3-C10-C9, “ = C5-C6-C7

same trend was observed in the C2-N1-C8. The C1-O1 in compound **DO** is noticeably shorter than in all compounds due to the effect of the phenyl group in these compounds. The same was noticed for the N-C bond length, where it is remarkably shorter in **DO** compared to the others. The negative hyper-conjugative effect of lone pair in the nitrogen atom toward the carbonyl contributed to the decrease in the N-C bond lengths. These results are in line with those observed in earlier studies by Jiménez-Cruz et al. [18].

Vibrational Frequencies

The IR spectra of molecules were calculated in the range of 0–4000 cm^{-1}. Comparison of the calculated and experimental results show a relatively good agreement despite that the experimental values were recorded in the solid state while the calculated values were studied in the gas phase [13]. However, overestimation of some frequencies was noticed, such as the ν O-H stretching of **HBD**. Future works are needed to address these overestimations and to investigate further effects such as solvation. Table 2 shows the IR data of the experimental and calculated values of studied molecules. In the case of compound **BD** that was chosen as a model of these series, experimentally [13] absorption bands were shown at 2952 cm^{-1} (ν C-H, benzene), 1464 cm^{-1} (ν C=C, benzene), 880 cm^{-1} (ν C-H, benzene), 1707 cm^{-1} (ν C=O, ketone), 1605 cm^{-1} (ν Ph), which almost coincide with those of maxima obtained theoretically, as shown in Fig. 2.

Generally, in the region of 1680-1730 cm^{-1}, the carbonyl C=O stretching vibrations are observed. In the case of compound **BD,** this band was obtained as a strong band at 1689 cm^{-1}. The band of stretching phenyl (ν Ph) group was noticed in the region of 1550–1650 cm^{-1}. Calculated spectra of the studied compounds can be provided upon request.

Molecular Orbital Energies (HOMO and LUMO Analyses)

The frontier molecule orbitals (FMOs) which refer to the HOMOs and LUMOs, have an important role in

Table 2. FT-IR data of the experimental [13] (and calculated) values of **BD**, **HBD**, **MBD**, and **HMBD**

Compound	ν C=O, ketone/cm^{-1}	ν Ph/cm^{-1}	ν O-H/cm^{-1}	ν OCH3/cm^{-1}
BD	1707 (1689)	1605 (1637)	-	-
HBD	1704 (1686)	1600 (1646)	3200 (3600)	-
MBD	1713 (1682)	1609 (1632)	-	1251, 1127 (1250, 1172)
HMBD	1706 (1680)	1569 (1561)	3396 (3600)	1270, 1145 (1270, 1168)

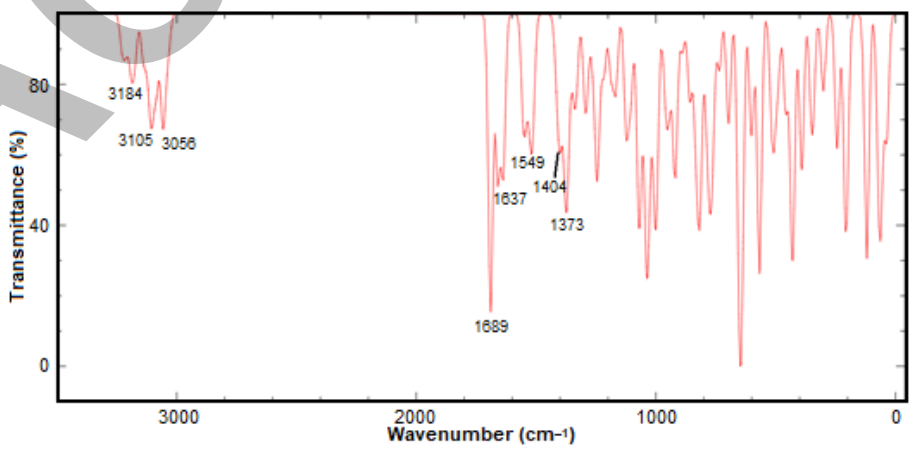

Fig 2. Calculated IR spectra of **BD** in the frequency range of 0–3300 cm^{-1}

chemical reactions, molecular electronic and physiochemical properties such as ionization potential, electron affinity, chemical reactivity, kinetic stability, electronegativity, and electrophilicity [19-20]. The calculated HOMOs and LUMOs of the titled molecules are shown in Fig. 3. Table 3 shows the electronic characteristics calculated for the given molecules: the frontier orbital energies (E_{homo}, E_{lumo}), the zero-point energy (ZPE), and the entropy (S) and final total energy (E_{final}). Generally, the results showed a decrease in final energy of optimized structures as follows: **A** > **D** > **DO** > **BD** > **HBD** > **MBD** > **HMBD**. The results also showed the same trend in the energy of E_{HOMO} and E_{LUMO}; an increase in the energy of E_{HOMO} and a decrease in the energy of E_{LUMO}. This is attributed to the effect of the replacement of carbon atoms with good donor atoms such as nitrogen and oxygen through comparison between molecules **A** and **D**.

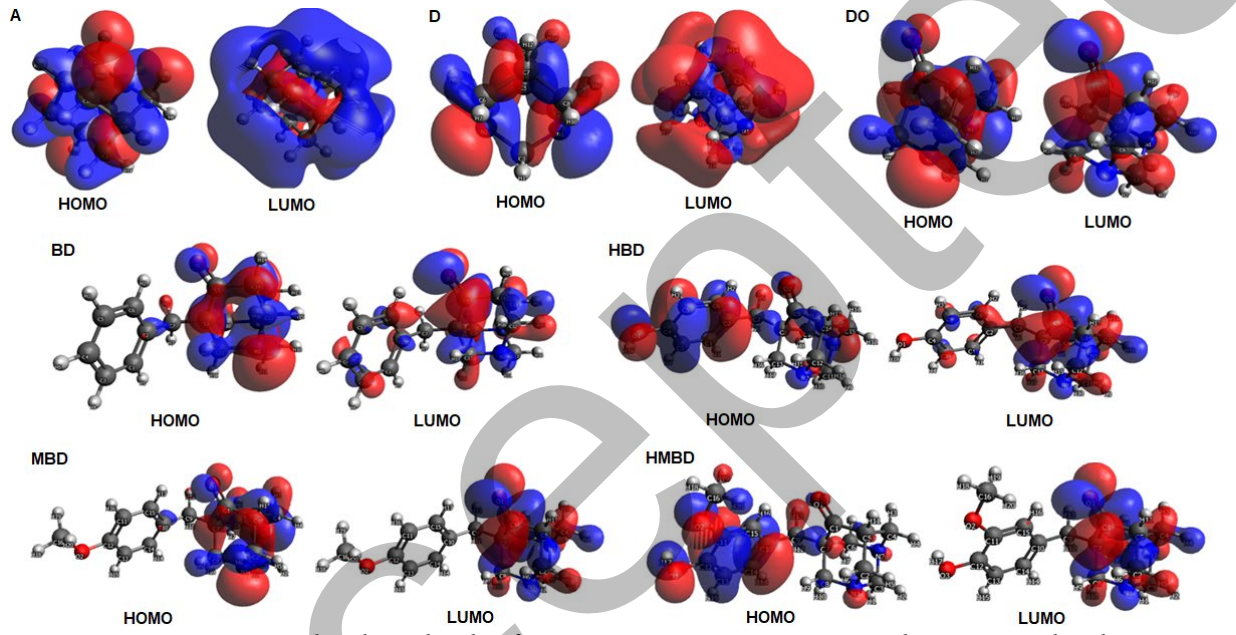

Fig 3. Frontier molecular orbitals of **A**, **D**, **DO**, **BD**, **HBD**, **MBD**, and **HMBD** molecules

Table 3. Calculated basic electronic energy characteristics of the studied compounds at room temperature (298.15 K)

Compound	E_{final}, a.u. (E_{final} kcal/mol)	E_{HOMO}, eV	E_{LUMO}, eV	S, cal/(mol K)	ZPE, kcal/mol
A	-390.348 (-244947.53)	-7.525	2.414	81.192	154.291
D	-422.359 (-265034.71)	-5.217	1.215	80.259	139.339
DO	-496.320 (-311446.10)	-5.797	-0.358	85.088	126.765
BD	-766.448 (-480954.36)	-5.784	-0.526	114.764	196.305
HBD	-841.608 (-528117.68)	-5.745	-0.478	119.739	198.515
MBD	-880.873 (-552756.73)	-5.721	-0.451	126.422	216.776
HMBD	-956.036 (-599922.67)	-5.382	-0.492	132.372	219.081

Table 4. Ionization potential **(IP)**, electron affinity **(EA)** and electronegativity **(X)** values of the studied compounds

Compound	$E_{HOMO-LUMO}$ gap/eV	IP/eV	EA/eV	X/eV
A	9.939	7.525	-2.414	2.5555
D	6.432	5.217	-1.215	2.001
DO	5.439	5.797	0.358	3.0775
BD	5.258	5.784	0.526	3.155
HBD	5.267	5.745	0.478	3.1115
MBD	5.27	5.721	0.451	3.086
HMBD	4.89	5.382	0.492	2.937

When comparing molecule **D** with **DO**, where C=O is introduced, it is clear that the energy E_{HOMO} is slightly decreased. While in the case of molecules **BD**, **HBD**, **MBD**, **HMBD** compared with molecule **A**, changes in the energy of E_{HOMO} and E_{LUMO} are the result from the introduction of the π-system (phenyl group) and donor groups. It is well known that the high value of the E_{HOMO} indicates a strong donor molecule, while the low value of the E_{LUMO} is likely referring to a good acceptor molecule to form stable bonds.

Electronic Properties: HOMO-LUMO Gap Energy ($E_{HOMO-LUMO}$ Gap), Electron Affinity (EA), Ionization Potential (IP), and Electronegativity (X)

The HOMO-LUMO gap energy (**$E_{HOMO-LUMO}$ gap**), Ionization potential (**IP**), electron affinity (**EA**) and electronegativity (**X**) were calculated by using the B3LYP with 6-31G level of theory for the titled molecules, as described in Computational Methods. Table 4 presents the calculated HOMO-LUMO gap energy (**$E_{HOMO-LUMO}$ gap**), Ionization potential (**IP**), electron affinity (**EA**), and electronegativity (**X**) values of the titled molecules calculated using equations 1-4. Generally, when comparing the titled molecules, the $E_{HOMO-LUMO}$ gap is changed as follows: **A** > **D** > **DO** > **BD** < **HBD** < **MBD** > **HMBD**. It is known that IPs and EAs are closely related to the energies of HOMO and LUMO, respectively. It can be seen from Table 4 that the highest IP value is for **A** indicating the more stable molecule with inertness in chemical reactivity. Meanwhile, the lowest IP value is for both **D** and **HMBD** due to the effect of the donor groups in these molecules, indicating more reactive molecules.

The calculated **EA** values of compound **A** and **D** are negative while for the rest of molecules are positive. A close look at these results, molecule **A** is more negative than that of molecule **D**. In the case of **BD**, **HBD**, **MBD**, and **HMBD,** the EA values are positive due to the presence of donor groups. From Table 4, it can also be noticed that the electronegativity (**X**) of the titled molecules are high (positive). These findings are important in many applications, such as corrosion inhibition. Further work is needed to investigate the properties of these materials as a corrosion inhibitor.

■ CONCLUSION

To sum up, the structure and physiochemical properties of Adamantane (**A**), 1,3-Diaza-adamantan (**D**), 1,3-Diaza-adamantan-6-one (**DO**), 5-Benzyl-1,3-diaza-adamantan-6-one (**BD**), 5-(4-Hydroxybenzyl)-1,3-diaza -adamantan-6-one (**HBD**), 5-(4-Methoxy benzyl)-1,3-diaza-adamantan-6-one (**MBD**), and 5-(4-Hydroxy-3-methoxybenzyl)-1,3-diaza-adamantan-6-one (**HMBD**) have been revealed at a relatively small basis set by using the DFT calculations with the hybrid B3LYP functional and 6-31G level of theory. The IR spectra of the titled molecules have been calculated in the gas phase. Moving from **A** to **HMBD**, a decrease in the values of LUMO and total energy are noticed, while the values of HOMO increase, indicating the more reactive molecule in the reactions with electrophiles with potential application as a corrosion inhibitor. These findings are supported by the decrease in the $E_{HOMO-LUMO}$ gap values, decrease in the values of **IP**, and increase in the values of **EA**.

■ REFERENCES

[1] Štimac, A., Šekutor, M., Mlinarić-Majerski, K., Frkanec, L., and Frkanec, R., 2017, Adamantane in drug delivery systems and surface recognition, *Molecules*, 22 (2), 297.

[2] Savel'eva, S.A., Leonova, M.V., Baimuratov, M.R., and Klimochkin, Y.N., 2018, Synthesis and transformations of aryl-substituted alkenes of the adamantane series, *Russ. J. Org. Chem.*, 54 (7), 996–1002.

[3] Ivleva, E.A., Tkachenko, I.M., and Klimochkin, Y.N.,

2017, Synthesis of adamantane functional derivatives basing on N-[(adamantan-1-yl)alkyl]acetamides, *Russ. J. Org. Chem.*, 52 (11), 1558–1564.

[4] Suslov, E., Zarubaev, V.V., Slita, A.V., Ponomarev, K., Korchagina, D., Ayine-Tora, D.M., Reynisson, J., Volcho, K., and Salakhutdinov, N., 2017, Anti-influenza activity of diazaadamantanes combined with monoterpene moieties, *Bioorg. Med. Chem. Lett.*, 27 (19), 4531–4535.

[5] Hickmott, P.W., Wood, S., and Murray-Rust, P., 1985, Introduction of pharmacophoric groups into polycyclic systems. Part 3. Amine derivatives of adamantane and diaza-adamantane, *J. Chem. Soc., Perkin Trans. 1*, 0, 2033–2038.

[6] Vrynchanu, N.A., Sergienko, O.V., and Maksimov Yu, N., 2009, Research of some sides of antifungal activity mechanism act of new adamantane derivative, *Морфологія*, 3 (2), 24–27.

[7] Schwertfeger, H., Fokin, A.A., and Schreiner, P.R., 2008, Diamonds are a chemist's best friend: Diamondoid chemistry beyond adamantane, *Angew. Chem. Int. Ed.*, 47 (6), 1022–1036.

[8] Gunawan, M.A., Hierso, J.C., Poinsot, D., Fokin, A.A., Fokina, N.A., Tkachenko, B.A., and Schreiner, P.R., 2014, Diamondoids: Functionalization and subsequent applications of perfectly defined molecular cage hydrocarbons, *New J. Chem.*, 38 (1), 28–41.

[9] Karthik, G., Sundaravadivelu, M., Rajkumar, P., and Manikandan, M., 2014, Diaza-adamantane derivatives as corrosion inhibitor for copper in nitric acid medium, *Res. Chem. Intermed.*, 41 (10), 7593–7615.

[10] Arutyunyan, G.L., Paronikyan, R.V., Saakyan, G.S., Arutyunyan, A.D., and Gevorkyan, K.A., 2008, Synthesis and reactions of polyhedral compounds. 29. Synthesis and antibacterial activity of 1,3-diazaadamantane derivatives, *Pharm. Chem. J.*, 42 (1), 18–22.

[11] Arutyunyan, G.L., Dzhagatspanyan, I.A., Nazaryan, I.M., Akopyan, A.G., and Arutyunyan, A.D., 2007, Synthesis and conversions of polyhedral compounds: 28. Synthesis and psychotropic activity of some 1,3-diazaadamantane derivatives, *Pharm. Chem. J.*, 41 (11), 591–593.

[12] Sharabi-Ronen, Y., Levinger, S., Lellouche, M.B., and Albeck, A., 2014, Anti-neoplastic activity of 1,3-diaza-2-functionalized-adamantan-6-one com pounds against melanoma cells, *Med. Chem.*, 10 (1), 27–37.

[13] Kuznetsov, A.I., Alasadi, R.T., Senan, I.M., and Serova, T.M., 2014, Synthesis of fragrant 1,3-diazaadamantan-6-ones, *Russ. Chem. Bull.*, 63 (9), 2195–2197.

[14] Gordon, M.S., and Schmidt, M.W., 2005, "Advances in electronic structure theory: GAMESS a decade later" in *Theory and Applications of Computational Chemistry: The first forty years*, Eds., Dykstra, C., Frenking, G., Kim, K., and Scuseria, G., 1st Ed., Elsevier Science, Amsterdam, 1167–1189.

[15] Becke, A.D., 1993, A new mixing of Hartree–Fock and local density-functional theories, *J. Chem. Phys*, 98 (2), 1372.

[16] Fernández, M.J., Gálvez, E., Lorente, A., Camuñas, J.A., Sanz, J., and Fonseca, I., 1990, Synthesis, structural and conformational study of 6-hydroxy (or acyloxy) derivatives of the 1,3-dimethyl-1,3-diazoniatricyclo[3.3.1.1$^{3-7}$]decane system, *J. Heterocycl. Chem.*, 27 (5), 1355–1359.

[17] Hanwell, M.D., Curtis, D.E., Lonie, D.C., Vandermeersch, T., Zurek, E., and Hutchison, G.R., 2012, Avogadro: An advanced semantic chemical editor, visualization, and analysis platform, 2012, *J. Cheminform.*, 4 (1), 17.

[18] Jiménez-Cruz, F., Ríos-Olivares, H., and Gutiérrez, J.L.G., 2005, "Molecular structure in 1-azaadamantanes and 1,3-diazaadamantanes" in *Structural Analysis of Cyclic Systems*, Eds., Iriepa, I., Research Signpost, Trivandum, India, 101–125.

[19] Parr, R.G., Donnelly, R.A., Levy, M., and Palke, W.E., 1978, Electronegativity: The density functional viewpoint, *J. Chem. Phys.*, 68 (8), 3801.

[20] Figueredo, S., Páez, M., and Torresbc, F., 2019, The electrophilic descriptor, *Comput. Theor. Chem.*, 1157, 34–39.